Electronic Supplementary Material (ESI) for Journal of Materials Chemistry B.

Modulation of Acetylcholinesterase Activity Using Molecularly Imprinted Polymer Nanoparticles

Sergey Piletsky, Thomas S Bedwell, Rachele Paoletti, Kal Karim, Francesco Canfarotta, Rachel Norman, Donald J L Jones, Nicholas W Turner and Elena Piletska

Correspondence to: Elena Piletska (ep219@le.ac.uk)

This PDF file includes:

Supplementary Figures

Supplementary Data Tables

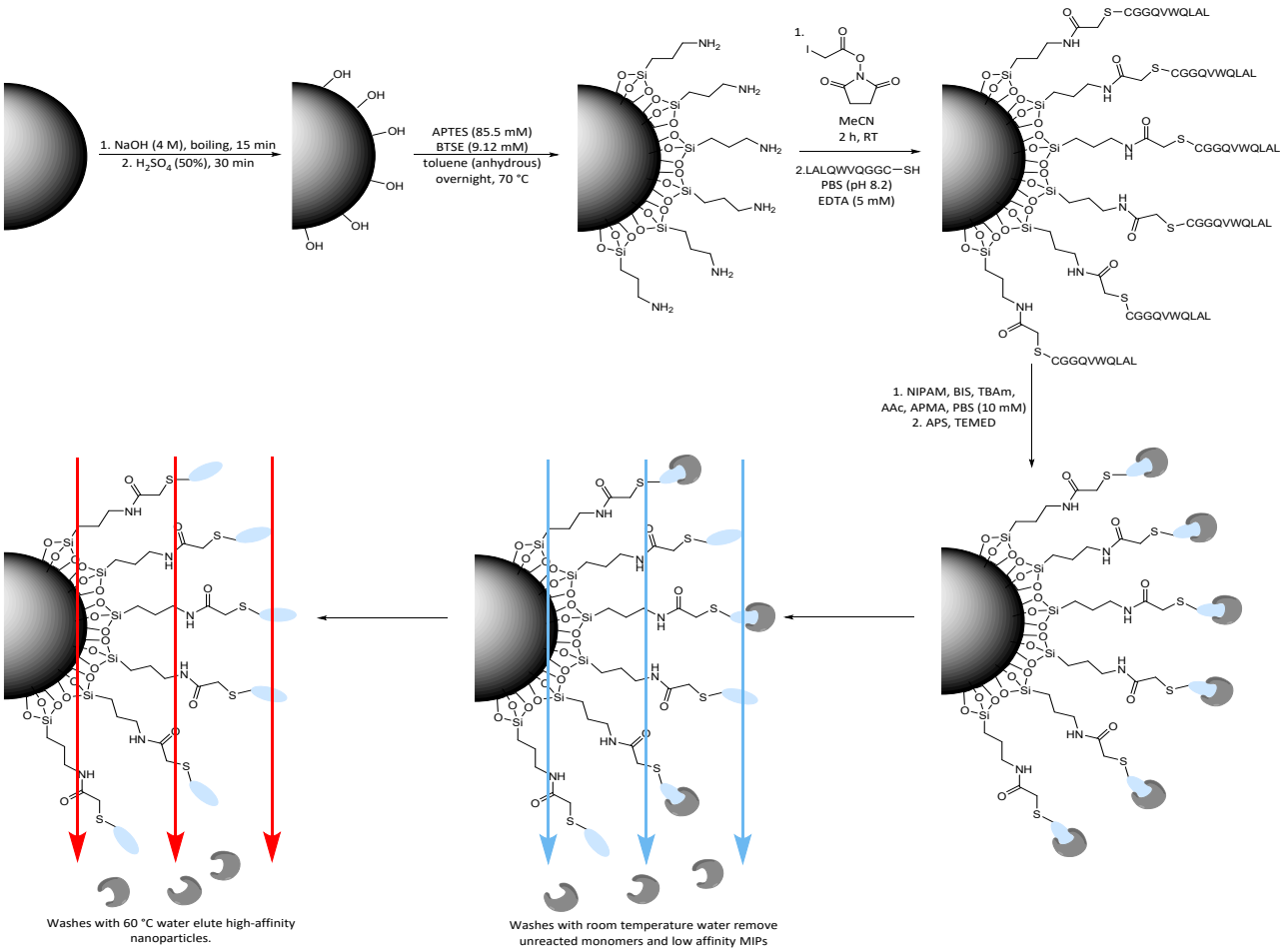

Fig. S1. Solid phase synthesis of MIP nanoparticles.

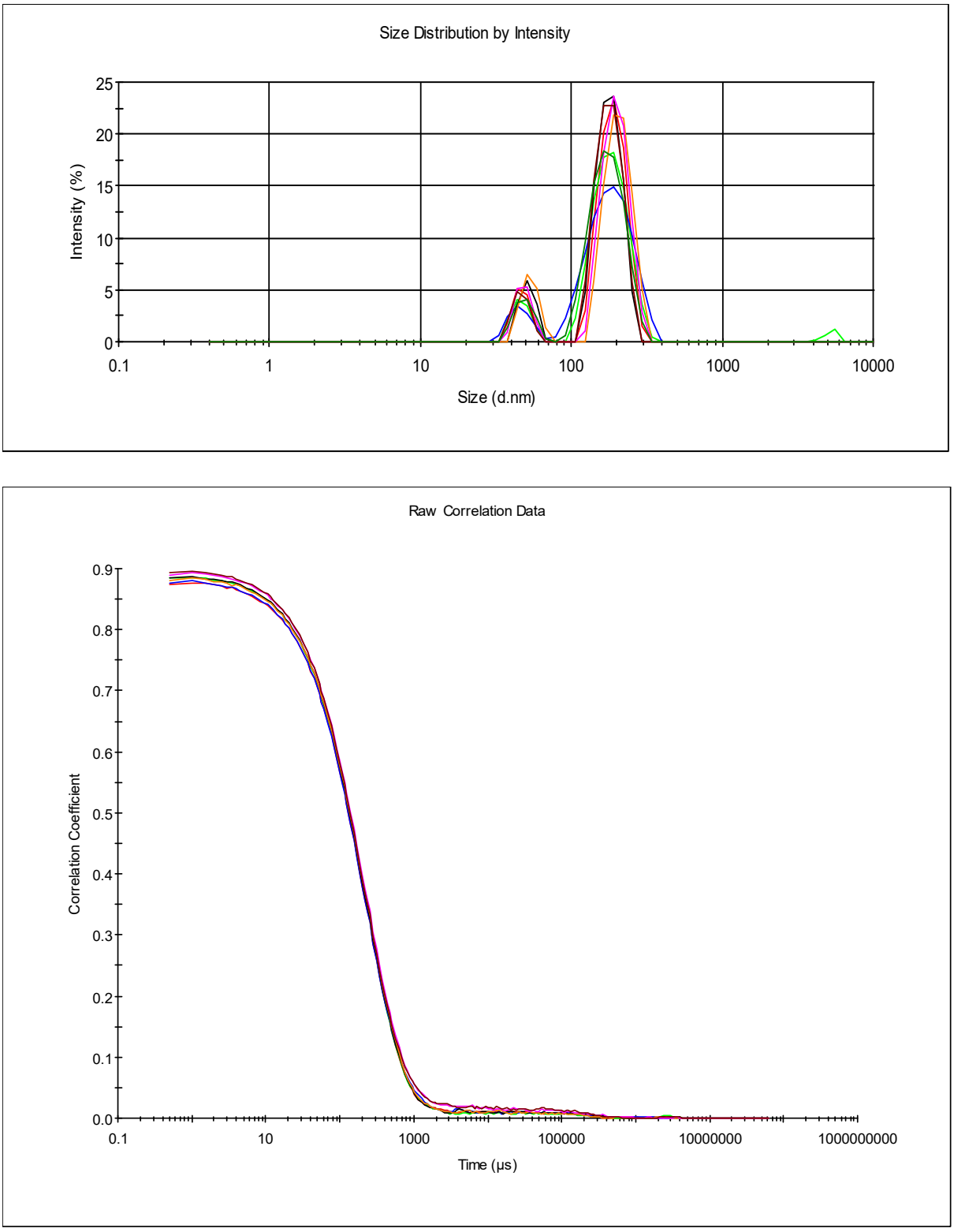

Fig. S2. Size distribution by intensity (top) and correlograms (bottom) for YWA-MIPs synthesized in this work (for the size and distribution values, see Table S1).

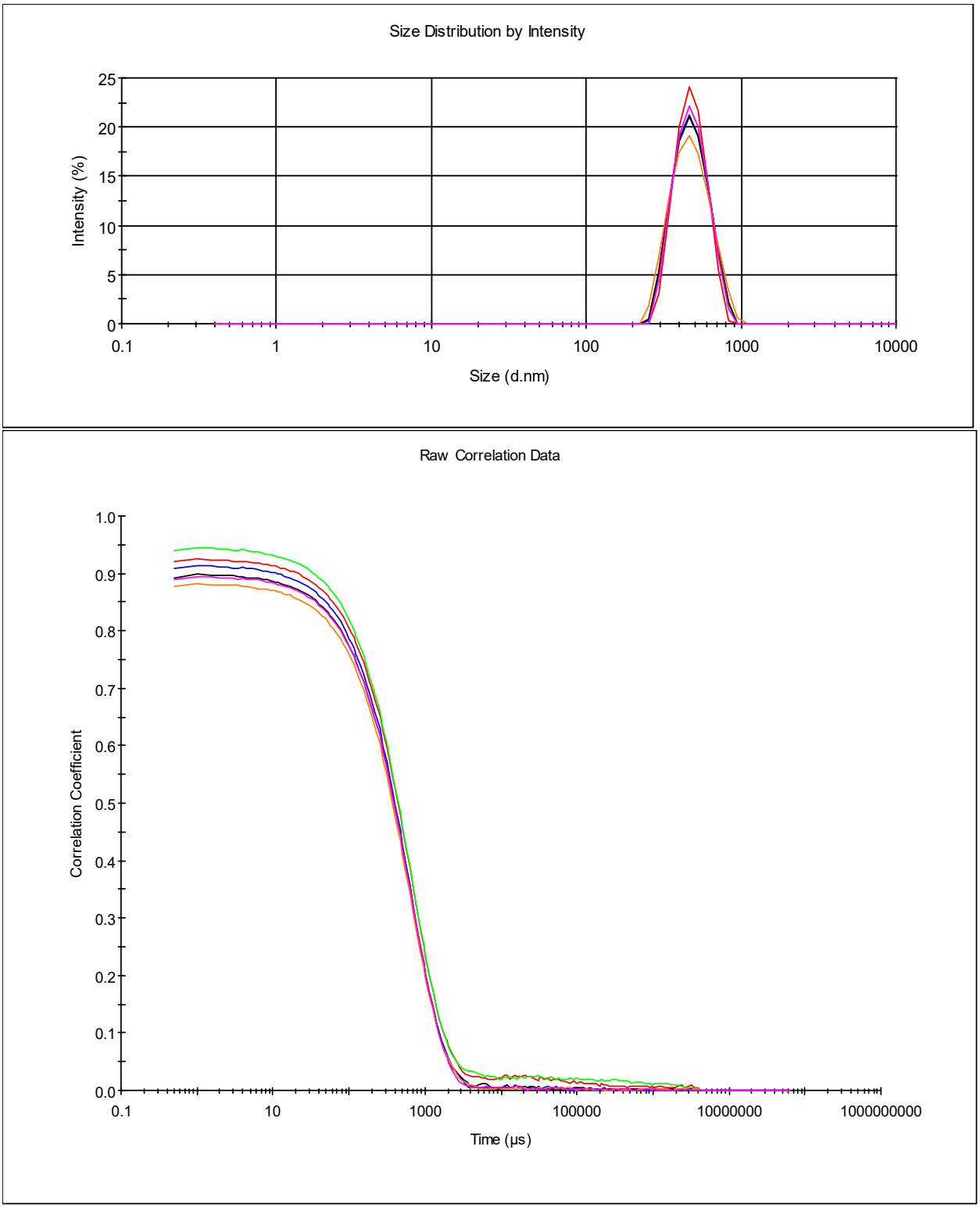

Fig. S3. Size distribution by intensity (top) and correlograms (bottom) for FRF-MIPs synthesized in this work (for the size and distribution values, see Table S1).

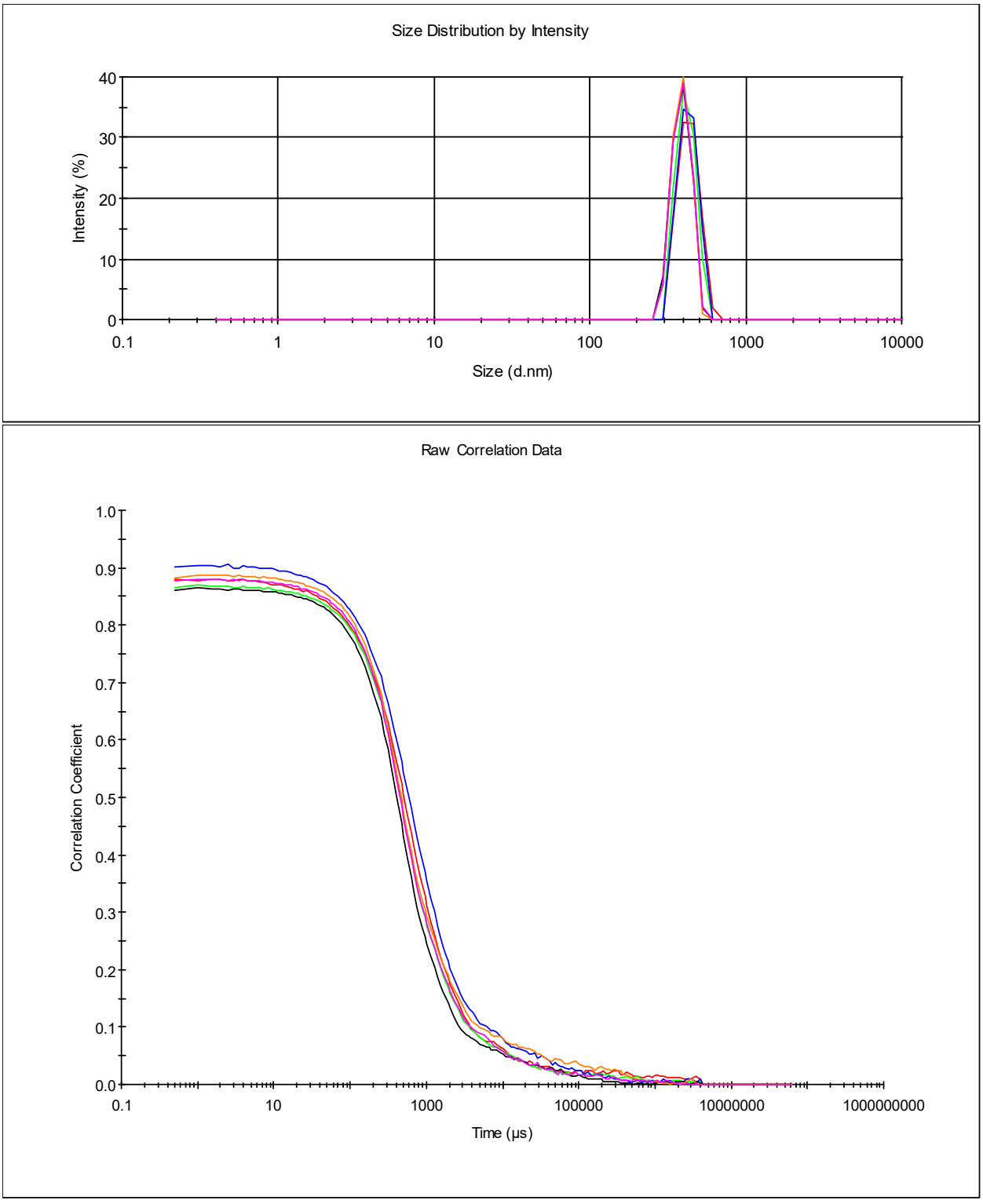

Fig. S4. Size distribution by intensity (top) and correlograms (bottom) for LAL-MIPs synthesized in this work (for the size and distribution values, see Table S1).

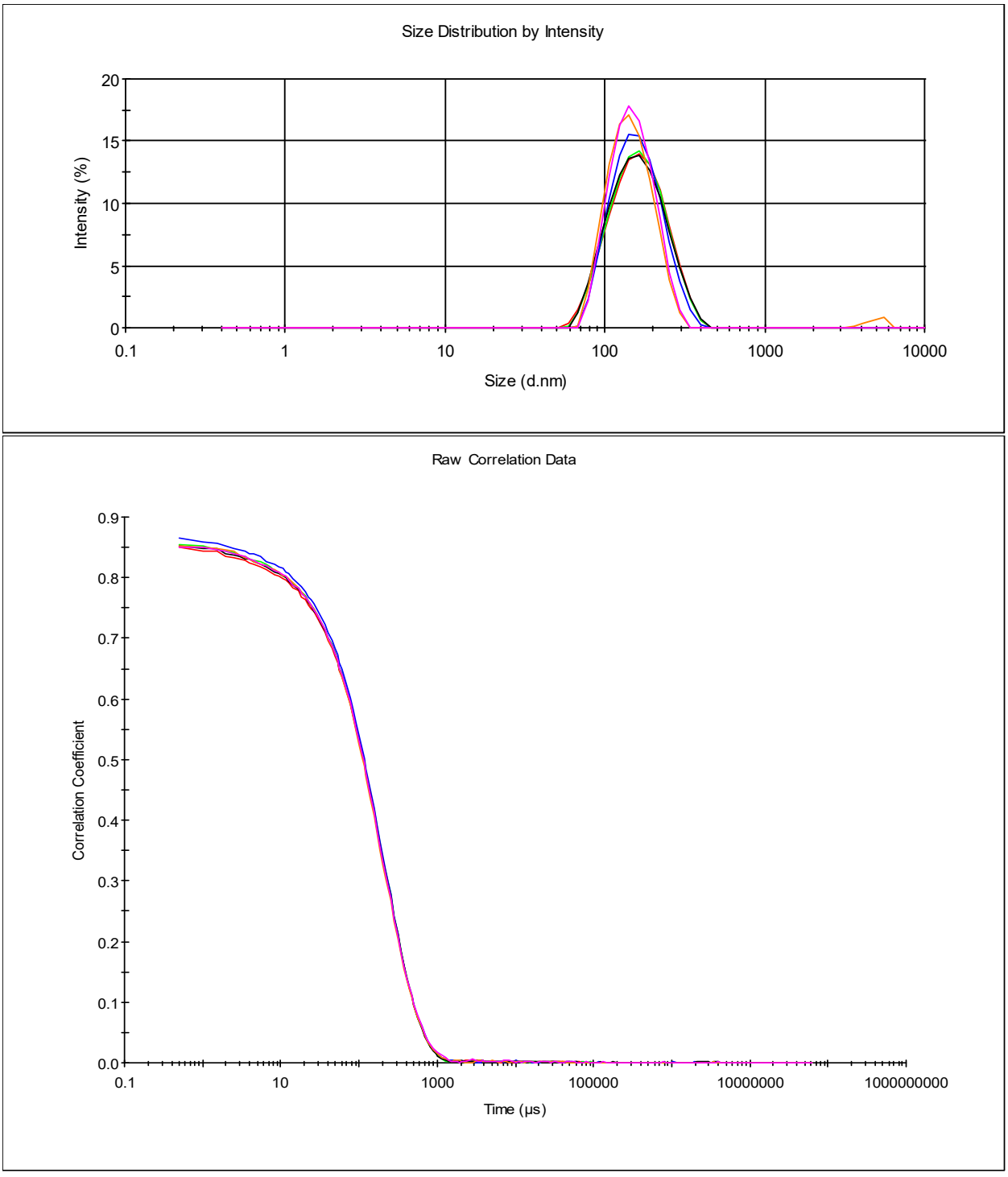

Fig. S5. Size distribution by intensity (top) and correlograms (bottom) for FGE-MIPs synthesized in this work (for the size and distribution values, see Table S1).

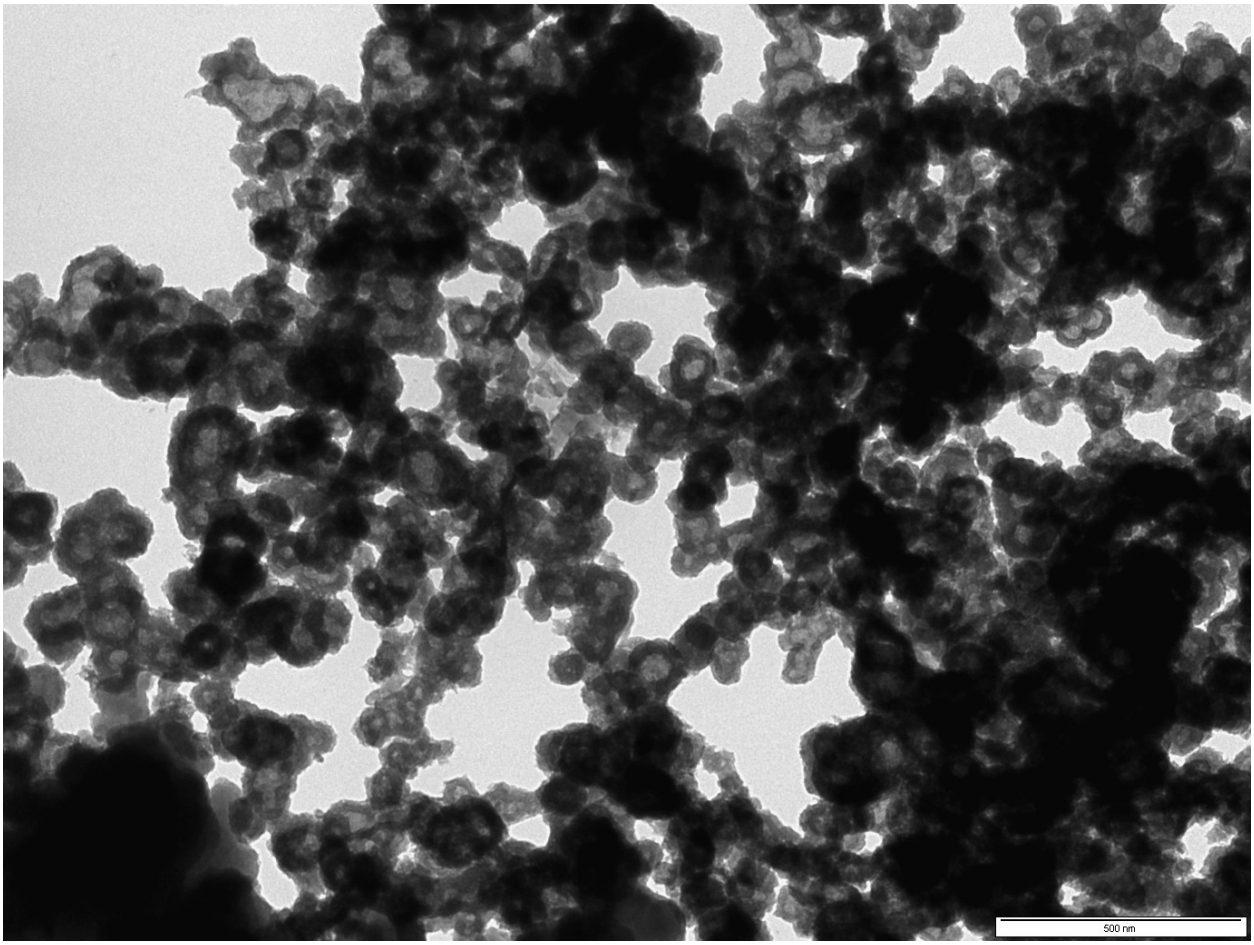

Fig. S6. Typical TEM image of the YWANFAR-specific MIP NPs specific for AChE.

Table S1: Size values and distribution for the nanoMIPs measured using DLS.

MIP	Size by intensity (d. nm)	Pdi	Number mean (d. nm)
LAL	408.4 ± 20.52	0.439 ± 0.056	393.6 ± 18.87
YWA	189.5 ± 10.52	0.304 ± 0.032	44.81 ± 2.86
FRF	484.3 ± 1.818	0.102 ± 0.047	431.1 ± 7.04
FGE	163.5 ± 9.381	0.140 ± 0.016	101.5 ± 6.76

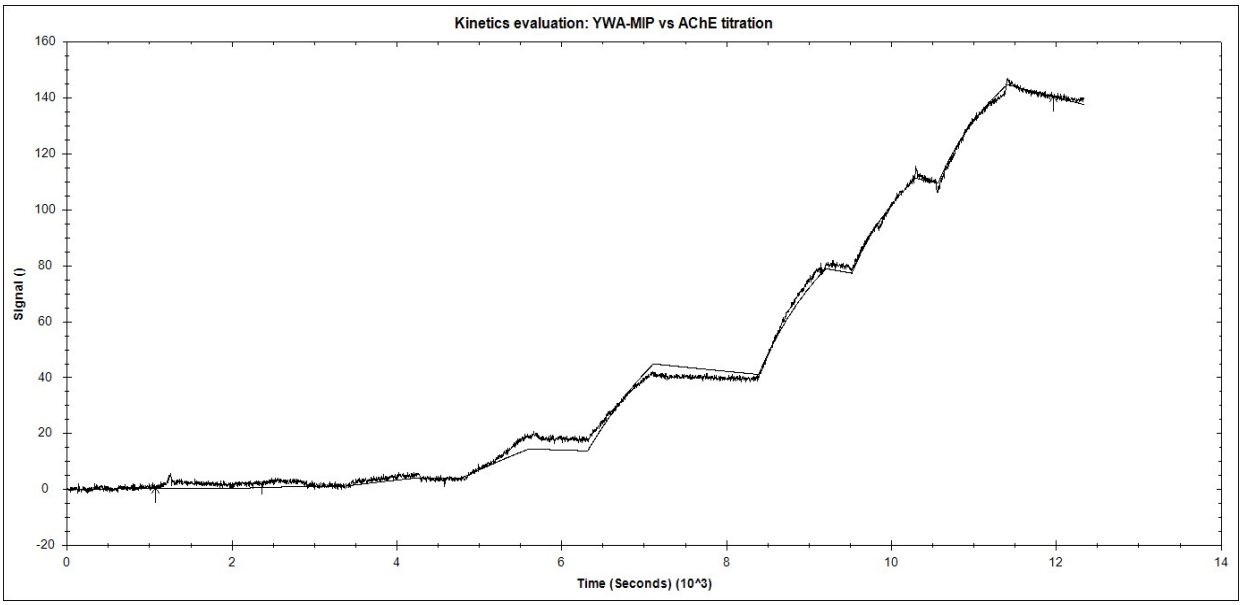

Fig. S7. SPR sensorgrams showing response of YWA-MIPs to injections of different concentrations of AChE. A kinetic titration injection strategy was employed for these experiments due to the difficulty of surface regeneration. AChE was injected at 5 different concentrations from 0.1 nM to 1 µM and allowed to associate and dissociate for 14 min and 5 min respectively, before a final dissociation of 120 min (not shown). All data were reference subtracted against a control polymer of the same monomer composition, and fit to a 1:2 interaction model using Tracedrawer 1.8 software.

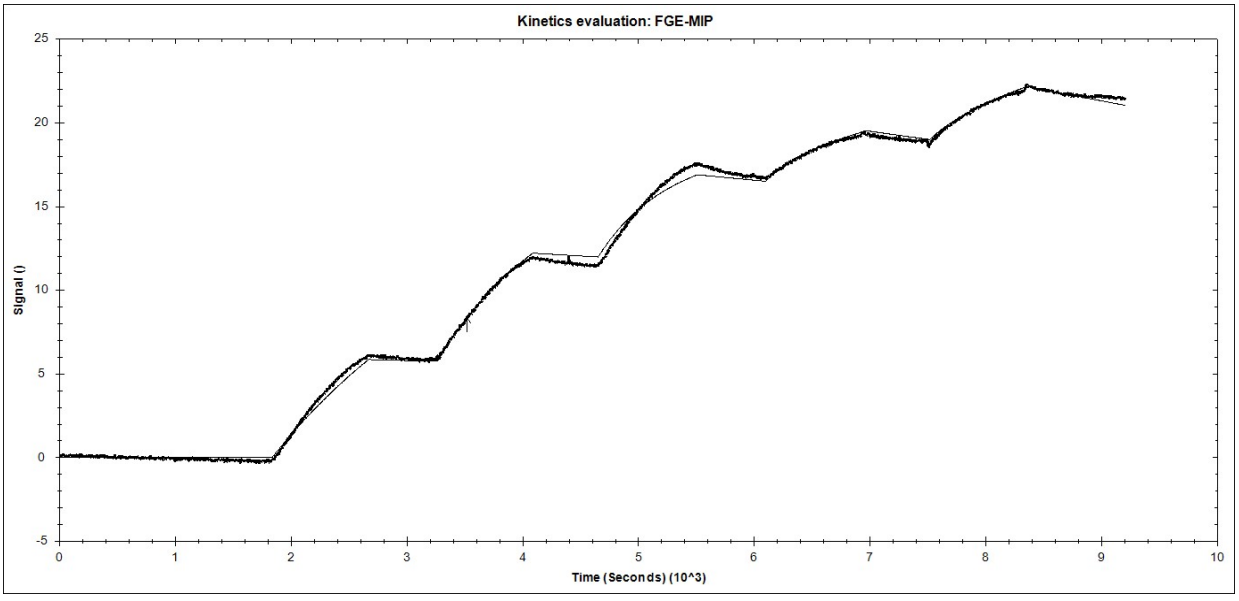

Fig. S8. SPR sensorgrams showing response of FGE-MIPs to injections of different concentrations of AChE. A kinetic titration injection strategy was employed for these experiments due to the difficulty of surface regeneration. AChE was injected at 5 different concentrations from 0.1 nM to 1 µM and allowed to associate and dissociate for 14 min and 5 min respectively, before a final dissociation of 120 min (not shown). All data were reference subtracted against a control polymer of the same monomer composition, and fit to a 1:2 interaction model using Tracedrawer 1.8 software.

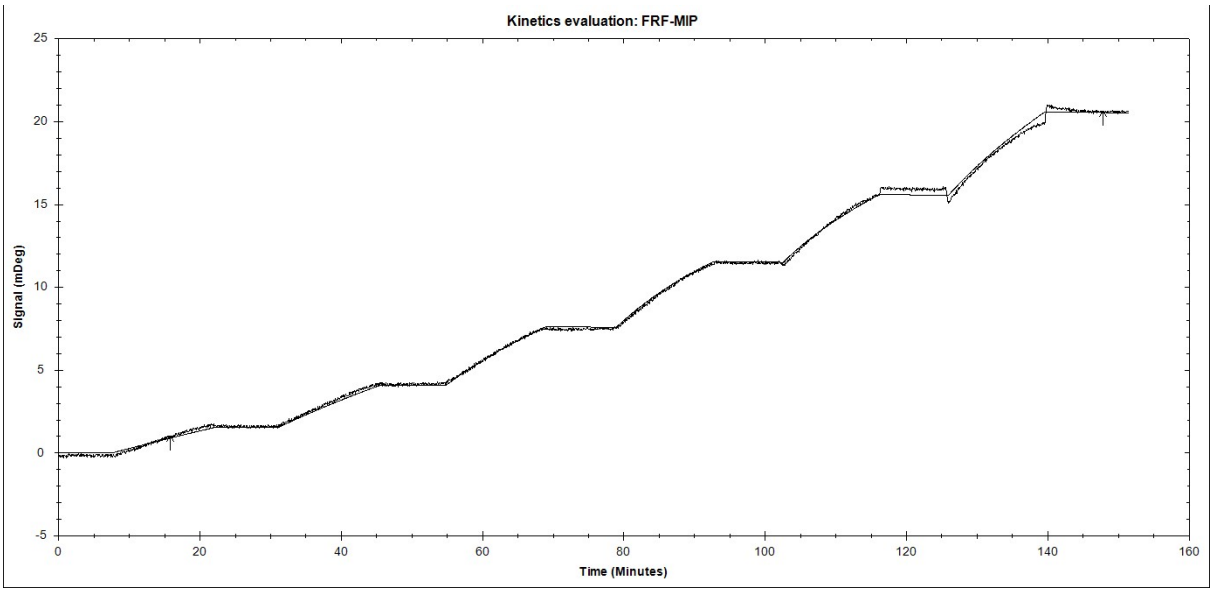

Fig. S9. SPR sensorgrams showing response of FRF-MIPs to injections of different concentrations of AChE. A kinetic titration injection strategy was employed for these experiments due to the difficulty of surface regeneration. AChE was injected at 5 different concentrations from 0.1 nM to 1 µM and allowed to associate and dissociate for 14 min and 5 min respectively, before a final dissociation of 120 min (not shown). All data were reference subtracted against a control polymer of the same monomer composition, and fit to a 1:2 interaction model using Tracedrawer 1.8 software.

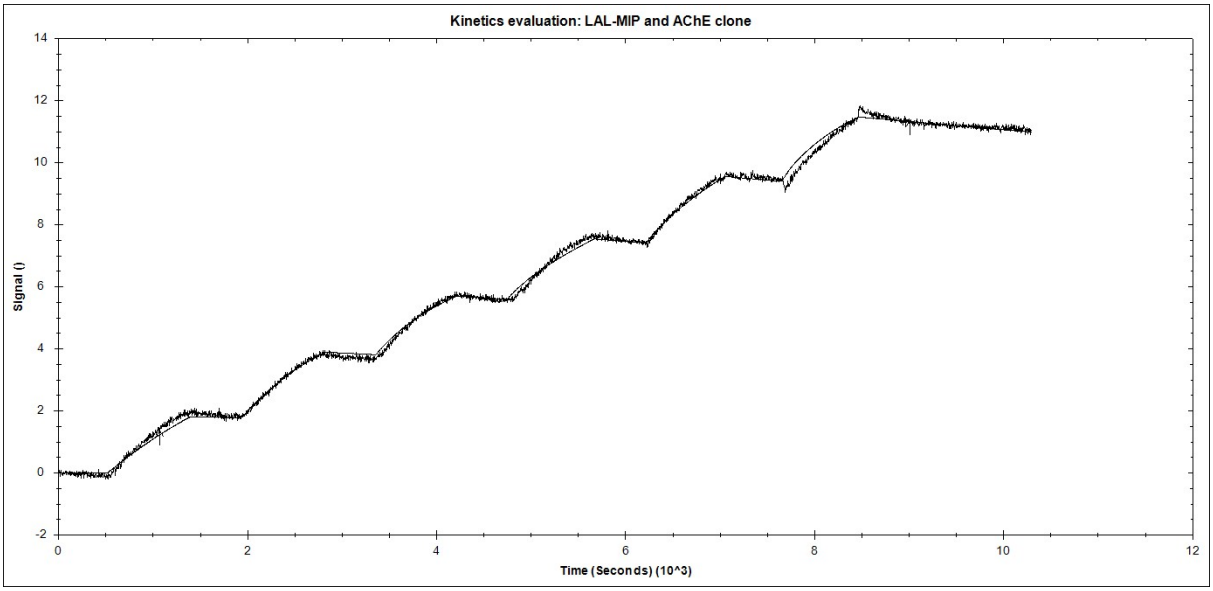

Fig. S10. SPR sensorgrams showing response of LAL-MIPs to injections of different concentrations of AChE. A kinetic titration injection strategy was employed for these experiments due to the difficulty of surface regeneration. AChE was injected at 5 different concentrations from 0.1 nM to 1 µM and allowed to associate and dissociate for 14 min and 5 min respectively, before a final dissociation of 120 min (not shown). All data were reference subtracted against a control polymer of the same monomer composition, and fit to a 1:2 interaction model using Tracedrawer 1.8 software.

Table S2. Affinity coefficient (K_D) of the synthesized MIP nanoparticles upon interaction with EeAChE enzyme measured using SPR.

Epitope used as template	K_D, nM	Chi^2
YWANFAR (YWA-MIP)	12.0	4.03
QVTIFGESAGAASVGM-HLLSPDSRPK (FGE-MIP)	78.6	0.06
FRFSFVPV (FRF-MIP)	0.40	0.03
LALQWVQDNIHFFGGNPK (LAL-MIP)	2.20	0.02

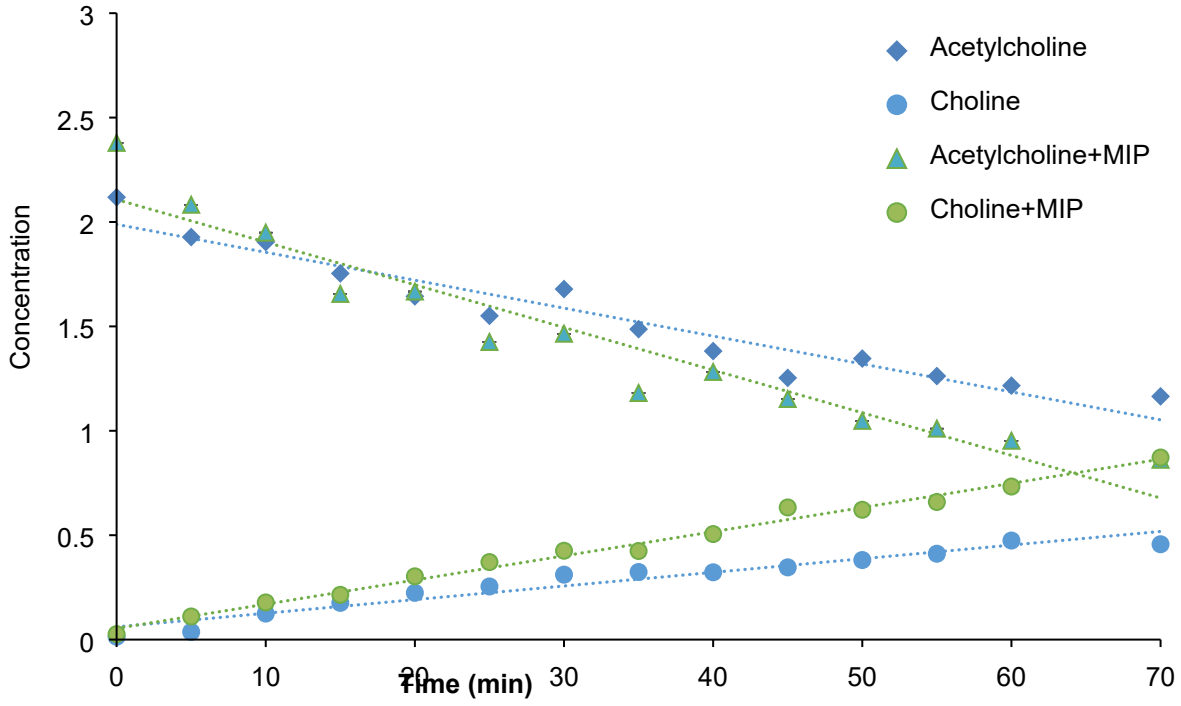

Fig. S11. Direct measure of substrate conversion by enzyme alone and in the presence of FRF-MIP.

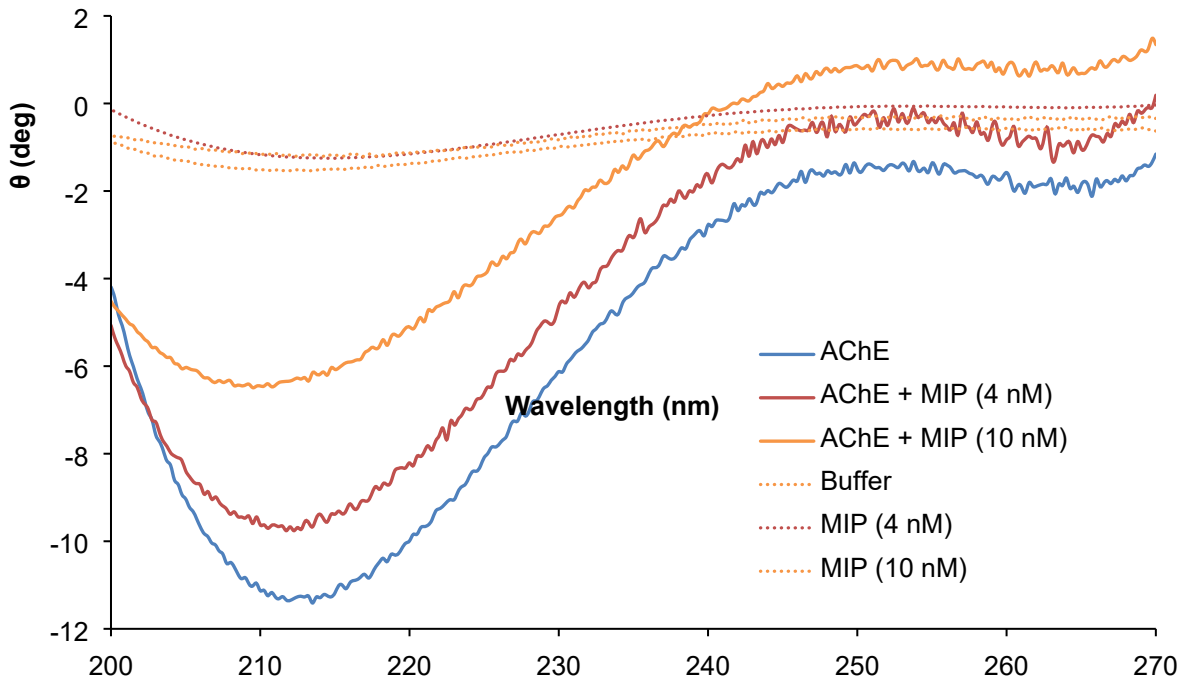

Fig. S12. Circular dichroism spectra of AChE with increasing concentration of YWA-MIP. Dashed lines correspond to control measurements of MIP without protein. Note that the nanoMIP materials appear to be inert spectroscopically.

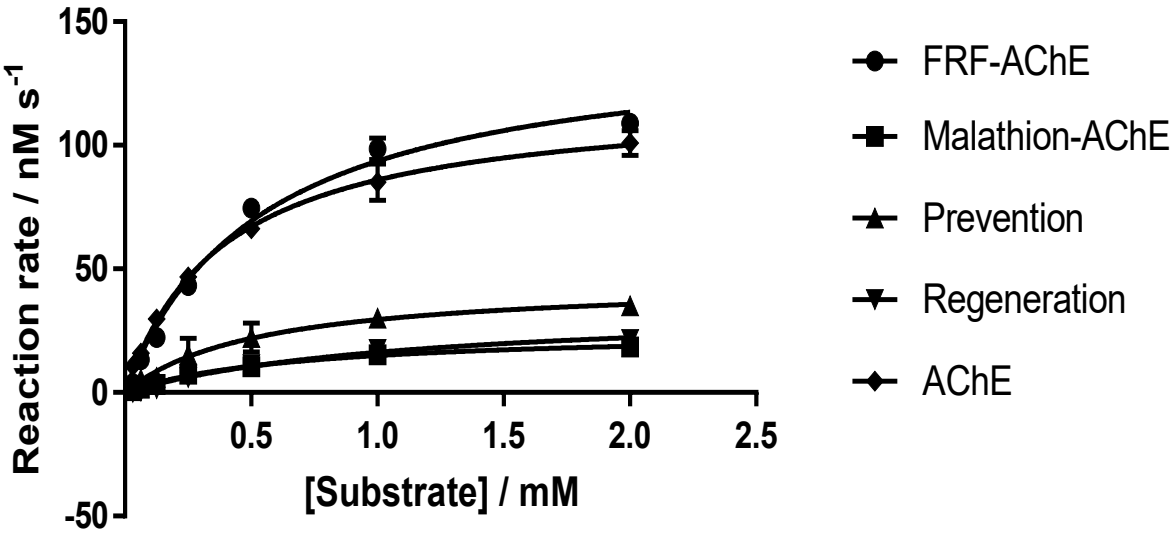

Fig. S13. Michaelis-Menten plot obtained for FRF-MIP. Error bars indicate SD. N=3

Table S3. Values obtained from Michaelis-Menten plot for FRF-MIP.

	FRF-MIP- AChE	Malathion-AChE	Prevention	Regeneration	AChE
Michaelis-Menten					
Best-fit values					
Vmax	143.9	25.01	45.12	34.92	119.7
Km	0.5378	0.674	0.5301	1.147	0.3928
Std. Error					
Vmax	6.829	1.315	4.506	4.047	3.342
Km	0.06444	0.08344	0.1343	0.2637	0.03039
95% CI (profile likelihood)					
Vmax	130.8 to 159.4	22.45 to 28.15	36.93 to 57.09	28.23 to 45.9	112.7 to 127.5
Km	0.4222 to 0.6895	0.5203 to 0.8828	0.3127 to 0.9282	0.7399 to 1.902	0.3313 to 0.4664
Goodness of Fit					
Degrees of Freedom	12	12	12	12	12
R square	0.9863	0.9867	0.9372	0.9714	0.9924
Absolute Sum of Squares	295.1	7.575	131.4	25.55	110.8
Sy. x	4.959	0.7945	3.309	1.459	3.038
Constraints					
Km	Km > 0	Km > 0	Km > 0	Km > 0	Km > 0
Number of points					
# of X values	14	14	14	14	14
# Y values analyzed	14	14	14	14	14